Research Article

NEURAL REGENERATION RESEARCH
www.nrronline.org

Zebrafish optic nerve regeneration involves resident and retinal oligodendrocytes

Cristina Pérez-Montes[1, 2, 3], Rosalía Hernández-García[1], Jhoana Paola Jiménez-Cubides[1], Laura DeOliveira-Mello[4], Almudena Velasco[1, 3, 5], Rosario Arévalo[1, 3, 5], Marina García-Macia[3, 6, 7, *], Adrián Santos-Ledo[1, 2, 3, *]

https://doi.org/10.4103/NRR.NRR-D-24-00621

Date of submission: June 4, 2024

Date of decision: July 31, 2024

Date of acceptance: October 15, 2024

Date of web publication: October 22, 2024

From the Contents

Graphical Abstract

Zebrafish optic nerve regeneration is supported by two waves of oligodendrocyte differentiation

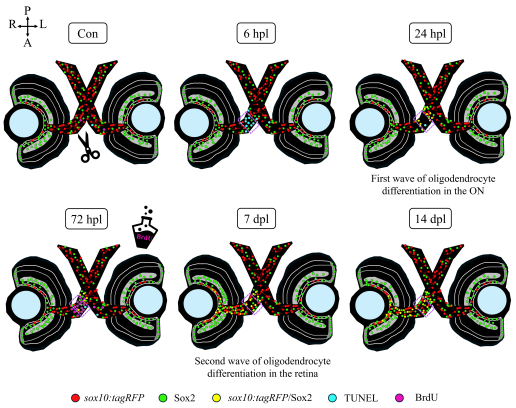

Abstract

The visual system of teleost fish grows continuously, which is a useful model for studying regeneration of the central nervous system. Glial cells are key for this process, but their contribution is still not well defined. We followed oligodendrocytes in the visual system of adult zebrafish during regeneration of the optic nerve at 6, 24, and 72 hours post-lesion and at 7 and 14 days post-lesion via the *sox10:tagRFP* transgenic line and confocal microscopy. To understand the changes that these oligodendrocytes undergo during regeneration, we used Sox2 immunohistochemistry, a stem cell marker involved in oligodendrocyte differentiation. We also used the Click-iT™ Plus TUNEL assay to study cell death and a BrdU assay to determine cell proliferation. Before optic nerve crush, *sox10:tagRFP* oligodendrocytes are located in the retina, in the optic nerve head, and through all the entire optic nerve. Sox2-positive cells are present in the peripheral germinal zone, the mature retina, and the optic nerve. After optic nerve crush, *sox10:tagRFP* cells disappeared from the optic nerve crush zone, suggesting that they died, although they were not TUNEL positive. Concomitantly, the number of Sox2-positive cells increased around the crushed area, the optic nerve head, and the retina. Then, between 24 hours post-lesion and 14 days post-lesion, double *sox10:tagRFP*/Sox2-positive cells were detected in the retina, optic nerve head, and whole optic nerve, together with a proliferation response at 72 hours post-lesion. Our results confirm that a degenerating process may occur prior to regeneration. First, *sox10:tagRFP* oligodendrocytes that surround the degenerated axons stop wrapping them, change their "myelinating oligodendrocyte" morphology to a "nonmyelinating oligodendrocyte" morphology, and die. Then, residual oligodendrocyte progenitor cells in the optic nerve and retina proliferate and differentiate for the purpose of remyelination. As new axons arise from the surviving retinal ganglion cells, new *sox10:tagRFP* oligodendrocytes arise from residual oligodendrocyte progenitor cells to guide, nourish and myelinate them. Thus, oligodendrocytes play an active role in zebrafish axon regeneration and remyelination.

Key Words: cell death; oligodendrocytes; optic nerve; proliferation; regeneration; Sox10; Sox2; visual system; zebrafish

Introduction

In zebrafish, Danio rerio, retinal neurogenesis continues after embryonic development by three different mechanisms: 1) preservation of a peripheral germinal zone (PGZ) at the circumferential edge of the retina, which provides all types of retinal cells, except rod photoreceptors; 2) rod progenitor proliferation in the outer nuclear layer of the central retina that intercalates into the extant retina; and (3) cells with proliferative capacity in the inner nuclear layer (INL), such as Müller cells (Bejarano-Escobar et al., 2014; Song et al., 2017). As a result, new retinal ganglion cell (RGC) axons are added, running throughout the optic nerve fiber layer (ONFL). Nascent axons from new RGCs grow towards the optic nerve head (ONH), where they converge to form the optic nerve (ON). This continuous growth allows the visual system of fish to regenerate after suffering from a lesion, in contrast to mammals, whose axons have low regenerative capacity (Van Houcke et al., 2017; Ávila-Mendoza et al., 2024). Several studies have pointed out the participation of glial cells such as astrocytes and oligodendrocytes in nourishing, guiding, and myelinating the constantly added axons, but many questions remain (Garcia-Pradas et al., 2018; Hu et al., 2024; Shinozaki et al., 2024).

Oligodendrocytes myelinate axons in the central nervous system (CNS) of vertebrates, forming the myelin sheath required for the fast saltatory

[1]Institute of Neuroscience of Castilla y León (INCyL), Salamanca, Spain; [2]Department of Human Anatomy and Histology, University of Salamanca, Salamanca, Spain; [3]Institute for Biomedical Research of Salamanca (IBSAL), Salamanca, Spain; [4]Department of Anatomy, Faculty of Medicine, University of Helsinki, Helsinki, Finland; [5]Department of Cell Biology and Pathology, University of Salamanca, Salamanca, Spain; [6]Institute of Functional Biology and Genomics (IBFG), University of Salamanca/CSIC, Salamanca, Spain; [7]Department of Biochemistry and Molecular Biology, University of Salamanca, Salamanca, Spain

***Correspondence to:** Adrián Santos-Ledo, PhD, santosledo@usal.es; Marina García-Macia, PhD, marinagarciamacia@usal.es.
https://orcid.org/0000-0002-6814-0718 (Adrián Santos-Ledo); https://orcid.org/0000-0002-3908-9060 (Marina García-Macia)

Funding: *This study was supported by the Lanzadera TCUE and C2 program (Universidad de Salamanca) (to ASL); the Spanish National Research Council (CSIC) funded by the Junta de Castilla y León and co-financed by the European Regional Development Fund (ERDF "Europe drives our growth)": Internationalization Project "CL-EI-2021-08-IBFG Unit of Excellence", Grant (PID2022-138478OA-100) funded by MICIU/AEI/10.13039/501100011033 and, by FEDER, UE (to MGM); Junta de Castilla y León (SA225P23) and Gerencia Regional de Salud (2701/A1/2023) (to AV); and the Plan Especial Grado Medicina (USAL) (to CPM). MGM is a Ramón y Cajal researcher: Grant RYC2021-033684-I funded by MICIU/AEI/10.13039/501100011033 and, by European Union NextGenerationEU/PRTR.*

How to cite this article: *Pérez-Montes C, Hernández-García R, Jiménez-Cubides JP, DeOliveira-Mello L, Velasco A, Arévalo R, García-Macia M, Santos-Ledo A (2026) Zebrafish optic nerve regeneration involves resident and retinal oligodendrocytes. Neural Regen Res 21(2):811-820.*

conduction of nerve impulses (Hines, 2021). Oligodendrocytes originate from oligodendrocyte progenitor cells (OPCs). These cells present different transcription factors, including Olig2 (oligodendrocyte transcription factor 2), Sox2, and Sox10 (Sock and Wegner, 2021; Ulloa-Navas et al., 2021; Santos-Ledo et al., 2023). OPCs are very proliferative and mobile. They migrate long distances, searching for axons to finally ensheathe them (Masson and Nait-Oumesmar, 2023). Then, OPCs become myelinating oligodendrocytes and express markers such as Sox10 (Nawaz et al., 2013; Münzel et al., 2014). The Sox family is key for oligodendrocyte physiology. Sox2 controls proliferation and cell fate during visual system development (Mercurio et al., 2019, 2021; Santos-Ledo et al., 2023). Moreover, Sox10 plays an essential role during the terminal differentiation of oligodendrocytes in coordination with other factors involved in CNS development, such as oligodendrocyte transcription factor 1 (Olig1), myelin regulatory factor (MYRF) and transcription factor 4 (TCF4) (Pingault et al., 2022; Negintaji et al., 2023). These Sox transcription factors are essential for regulating nerve regeneration. For example, after peripheral nerve injury, Sox2 supports the activation and migration of myelinating Schwann cells in the peripheral nervous system, whereas Sox10 promotes Schwann cell myelination (Zhang et al., 2023b). The role of these transcription factors in the CNS is less clear.

With this work, we aimed to clarify the response of oligodendrocytes when axonal input is lost after ON crush, a well-established model for axonal degeneration. Upon crush, RGCs survive, and their axons reinnervate their respective targets in the optic tectum, leading to full recovery after 2–4 weeks (McDowell et al., 2004; Stella et al., 2021). We hypothesize that new oligodendrocytes arise first directly from stem cells in the ON. Later, regeneration is supported by stem cells within the retina. Using the transgenic line sox10:tagRFP, we analyzed the distribution of mature oligodendrocytes in the visual system at 6, 24, and 72 hours post-lesion (hpl) and at 7 and 14 days post-lesion (dpl). To explore the changes that these mature oligodendrocytes and new oligodendrocytes undergo, we analyzed the presence of the stem cell marker Sox2. Finally, we studied their morphological changes, death, and proliferation during regeneration.

Methods

Animals

We used 32 adult zebrafish (*Danio rerio*) specimens of the transgenic line tg (*sox10:tagRFP*; ZDB-TGCONSTRCT-150316-1) (Blasky et al., 2014). The transgenic line was kindly donated by Bruce Appel. The fish were subsequently bred in our colonies in INCyL (University of Salamanca, Spain). The animals were maintained in aquaria under a 12-hour light/dark cycle without food restrictions at 28.5 ± 1°C. We used animals of either gender between 1 and 1.5 years of age, with standard lengths of 1.5 and 2 cm.

All procedures followed the European Union Directive 86/609/EEC, Recommendation 2007/526/EC, and directive 2010/63 concerning the protection of animals used for scientific purposes. This is enforced by Spanish legislation 32/2007, 6/2013, 53/2013, and Orden ECC/566/2015. The ARVO statement for the use of animals in ophthalmic and vision research was also followed. The Bioethics Committee of the University of Salamanca approved all procedures (USAL CBE 30/07/08).

Experimental groups

The ON lesion was located in the right eye. A total of 32 specimens were sacrificed as follows: control (n = 8), 6 hpl (n = 4), 24 hpl (n = 4), 72 hpl (n = 8), 7 dpl (n = 4), and 14 dpl (n = 4).

Optic nerve crush

ON crush of adult zebrafish was performed as previously described (Liu and Londraville, 2003; Cameron et al., 2020; Stella et al., 2021; Pérez-Montes et al., 2023). The fish were anesthetized via immersion in 0.003% tricaine methanesulfonate (Sigma, Deisenhofen, Germany, MS-222). Injury was performed under a stereomicroscope (Leica Zoom 2000, Wetzlar, Germany) on an ice-cold surface. The temporal half of the right eye was pulled out of its orbit with forceps. The lateral rectus eye muscle was subsequently sectioned via scissors to expose the ON. The ON was crushed with another pair of forceps (0.3 Newtons for 3 seconds) (Liu et al., 2020). All the fish survived the procedure. The fish were then returned to a fish tank until sacrifice.

Tissue dissection and processing

Control and injured fish were subjected to endpoint anesthesia in tricaine methanesulfonate (MS-222) before sacrifice, according to Spanish and European laws. We dissected the entire brain, including the eyes joined by the ONs, with fine forceps in cold 0.1 M pH 7.1 phosphate-buffered saline (PBS) under a microscope.

The samples were fixed in 4% paraformaldehyde (PFA) in PBS overnight at 4°C. The tissues were then rinsed in PBS and cryoprotected in 10% sucrose in PBS overnight at 4°C. Then, the tissues were embedded in a solution containing 1.5% agar and 10% sucrose, and the blocks were cryoprotected in 30% sucrose in PBS until sectioning. Finally, to observe ONs and retinas simultaneously, 12 µm-thick horizontal sections were obtained with a cryostat (Leica CM1850). The sections were stored at –20°C.

Click-iT™ Plus terminal deoxynucleotidyl transferase dUTP nick-end labeling assay

Apoptotic cells were detected *in situ* via the Click-iT™ Plus terminal deoxynucleotidyl transferase dUTP nick-end labeling (TUNEL) assay (Thermo Fisher Scientific, C10617). This kit detects modified EdUTP (a dUTP modified with a small bioorthogonal alkyne moiety) incorporated by terminal deoxynucleotidyl transferase at the 3′-OH ends of fragmented DNA, a hallmark of apoptosis. Detection is based on a click reaction (Breinbauer and Köhn, 2003), a copper-catalyzed covalent reaction between an Alexa Fluor picolyl azide dye and an alkyne (Cu(I)).

5-Bromo-2′-deoxyuridine assay

Bromodeoxyuridine (5-bromo-2′-deoxyuridine, BrdU), a thymidine analog incorporated during DNA replication of the cell cycle, was used as a marker for proliferation. BrdU exposure was performed via immersion, as previously described (Perdikaris et al., 2023). Forty-eight hours after ON crush, the zebrafish were individually immersed in a fresh solution of 5 mM BrdU (Sigma) diluted in tank water for 24 hours. A control group exposed for 24 hours to BrdU was used to compare the results. The fish were then anesthetized with tricaine methanesulfonate (Sigma, MS-222) before sacrifice.

Immunohistochemistry

The sections were rinsed in PBS and pre-incubated in 5% normal donkey or goat serum (Sigma) in PBS with 0.2% Triton X-100 at room temperature for 90 minutes. For BrdU labeling, the sections were first treated with 2 N HCl in PBS for 12 minutes at 37°C and neutralized with 0.1 M $Na_2B_4O_7$ in distilled H_2O (pH 8.5) for 30 minutes at room temperature before pre-incubation. Primary antibodies (**Table 1**) were incubated overnight in PBS supplemented with 0.2% Triton X-100, the appropriate serum and 1% dimethyl sulfoxide (DMSO) at 4°C. The sections were washed in PBS, and then secondary antibodies were used for 90 minutes at room temperature in the dark (**Table 2**). Finally, after a few washes in PBS, the nuclei were counterstained with 4′,6-diamidino-2-fenilindol (DAPI; 1/10000; Sigma). The sections were mounted with Fluoromount-G® Mounting Medium (Invitrogen, Waltham, MA, USA). The RFP fluorescence was not reinforced.

Imaging and quantification

All images were obtained with a confocal microscope (Leica Stellaris inverted DMi8) using a 40x oil immersion objective. A 12 µm z-stack was automatically acquired, and several images were obtained from each region. These images were assembled using the LASX software (Leica). The images were stored as 1024 × 1024 pixels and 8-bit TIFF files. The acquired z-stacks were transformed into maximum intensity projections and arranged in (Fiji is just) ImageJ (v. 2.14.0/1.54f). The brightness and contrast were adjusted only for better visualization.

Sox10:tagRFP- and Sox2-positive cells were quantified with the Cell Counter plugin from (Fiji is just) ImageJ in the inner plexiform layer (IPL), ganglion cell layer (GCL) and ONFL of the retina, the ONH and two different zones of the ON [the first ON zone is close to the ONH and contains the crushed area, which we refer to as the pre-ON, and the second ON zone is posterior to the crushed area and close to the optic chiasm (OC), which we refer to as the post-ON)]. TUNEL- and BrdU-positive cells were also quantified manually using the Cell Counter plugin but only in the pre-ON of both ONs (right optic nerve, RON, and left optic nerve, LON). Three non-consecutive sections from four different animals in each group were used.

Table 1 | **The primary antibodies used for immunohistochemistry**

	Host	Supplier, Cat#, RRID	Dilution	Observations
Bromodeoxyuridine (5-bromo-2′-deoxyuridine)	Rat	Abcam, Cambridge, UK, ab6326, AB_305426	1:1000	Synthetic nucleoside analoggue to thymidine, used in cell proliferation assays
Calretinin	Mouse	Swant, Burgdorf, Switzerland, 6b3, AB_ 10000320	1:1000	Calcium binding protein
Sox2	Rabbit	Abcam, Cambridge, UK, ab97959, AB_2341193	1:500	Transcription factor

Table 2 | **The secondary antibodies used for immunohistochemistry**

	Host	Supplier, Cat#, RRID	Conjugated	Dilution
Anti-rabbit	Donkey	Sigma, Deisenhofen, Germany, SAB4600036, AB_2728116	Alexa 488	1:400
Anti-rat	Goat	Jackson ImmunoResearch, St. Thomas Place, Ely, UK, 112-225-143, AB_2338277	Cy2	1:250
Anti-mouse	Donkey	Thermo Fisher Scientific, Waltham, MA, USA, A32787, AB_2762830	Alexa 647	1:400

The fluorescence intensity of *Sox10:tagRFP* cells in the pre-ON area was analyzed using ImageJ (Fiji) as previously described (Beccari et al., 2023). Briefly, the background was subtracted via the "subtract background" tool (rolling ball radius 100 pixels). We then used the "polygon selections" tool to select an area of interest. A *sox10:tagRFP* threshold was established for each image. The ON areas and their corresponding thresholds were merged. Finally, the area, integrated density and mean gray value were measured. Three nonconsecutive sections from four different animals in each group were used. Adobe Photoshop CS6 (Adobe, Portland, OR, USA) was used to construct the figures.

Statistical analysis

GraphPad Prism 5 (GraphPad Software, Boston, MA, USA) was used to generate graphs (violin representation). Student's *t* test was used to compare two groups (i.e., right optic nerve [RON], *versus* left optic nerve [LON]), and one-way analysis of variance with Tukey's multiple comparison test was used to detect differences among all groups (i.e., the number of *sox10:tagRFP* oligodendrocytes at any specific timepoint). $P < 0.05$ was considered statistically significant.

Results

The present work aims to clarify the response of oligodendrocytes when axonal input is lost with a well-established model for axonal degeneration, ON crush, using the zebrafish transgenic line *sox10:tagRFP*. After crushing the ON, we describe the location and changes that fully differentiated oligodendrocytes undergo at different timepoints (6, 24 and 72 hpl, 7 and 14 dpl). We also analyzed the distribution pattern of Sox2 via immunohistochemistry to identify the putative de-differentiation process that oligodendrocytes might undergo and the response of OPCs. To facilitate visualization of the ON structure, we marked the RGC axon fibers with calretinin (CR).

sox10:tagRFP oligodendrocytes and Sox2-positive cells are distributed throughout the visual system

We first examined the general distribution of *sox10:tagRFP* oligodendrocytes and Sox2-positive cells ($Sox2^+$ cells) in the zebrafish visual (**Additional Figure 1**). In the control retina (**Additional Figure 1A** and **B**), *sox10:tagRFP* oligodendrocytes were observed in the GCL (**Additional Figure 1A** and **C**) but not in the PGZ (**Additional Figure 1B**), and they extended into the ONFL close to the ONH (**Additional Figure 1D**). Typically, *sox10:tagRFP* oligodendrocytes were arranged in rows of several cells. Sox2 presented a wide distribution in the adult retina. All PGZ-treated cells were positive for Sox2 (**Figure 1A** and **B**). In the central retina, $Sox2^+$ cells were found mainly in the INL and in the GCL (**Additional Figure 1A–D**). Some scattered $Sox2^+$ cells were also detected in the inner plexiform layer (IPL), the ONFL, and the outer nuclear layer (**Additional Figure 1C**). In the ONH, *sox10:tagRFP* oligodendrocytes were arranged in rows of several cells (**Additional Figure 1D**). In contrast, very few $Sox2^+$ cells were found in this area (**Additional Figure 1D**). In the ONH–ON transition zone (the region of the ON that consists of the transition between the ONH and the ON), we found *sox10:tagRFP* oligodendrocytes on the marginal sides of the ON, forming the glial limitans (**Additional Figure 1E**). $Sox2^+$ cells were intermingled between these *sox10:tagRFP* cells.

Finally, the rest of the ON (pre- and post-ON) presented *sox10:tagRFP* oligodendrocytes and $Sox2^+$ cells dispersed all along (**Additional Figure 1A**, **E** and **F**). We could not detect any specific pattern of distribution, but *sox10:tagRFP* oligodendrocytes seemed to be in the interior of the ON, and $Sox2^+$ cells were more marginally (**Additional Figure 1E** and **F**). *Sox10:tagRFP* oligodendrocytes were arranged in rows, but $Sox2^+$ cells appeared solitarily. We did not find any co-localization between *sox10:tagRFP* and Sox2.

Thus, *sox10:tagRFP* oligodendrocytes are usually found in well-differentiated areas of the nervous system, such as the mature retina, the ONH, and through all the ON to the optic tectum. Furthermore, Sox2, a marker for stem cells, is usually found in proliferative regions such as the PGZ and the exterior limits of the ON.

Fully differentiated oligodendrocytes disappear from the point of injury

To understand the behavior of fully differentiated oligodendrocytes (*Sox10:tagRFP*) and stem cells ($Sox2^+$) during regeneration, we first examined their distribution in the area between the retina and the crushed point during regeneration (**Figure 1**).

Immediately after damage, *sox10:tagRFP* oligodendrocytes and $Sox2^+$ cells distributed in the ONH–ON transition zone (the region of the ON that consists of the transition between the ONH and the ON) were maintained in all experimental groups (**Figure 1A–F**). $Sox2^+$ cells were intermingled between *sox10:tagRFP* oligodendrocytes on the margin of the ON, forming the glial limitans.

After crush in the most anterior portion of the ON (pre-ON), *sox10:tagRFP* oligodendrocytes decreased from the injured area (**Figure 1B** and **B'**, quantified in **Figure 1G**; control *versus* 24 hpl: $P < 0.001$). At 24 hpl, the number of *sox10:tagRFP* oligodendrocytes reached its minimum, with fewer than 50 cells per section (**Figure 1C** and **C'**, quantified in **Figure 1G**; 6 hpl *versus* 24 hpl: $P < 0.01$). At 72 hpl, the number of *sox10:tagRFP* oligodendrocytes started to recover (**Figure 1D** and **D'**, quantified in **Figure 1G**; control *versus* 72 hpl: $P < 0.01$; 6 hpl *versus* 72 hpl: $P < 0.05$) and stabilized by 14 dpl, similar to the control (**Figure 1E–F'**, quantified in **Figure 1G**; 24 hpl and 72 hpl *versus* 14 dpl: $P < 0.0001$). Changes in the $Sox2^+$ population were less dramatic. We did not detect any variations in the number of $Sox2^+$ cells between 6 hpl and 7 dpl (**Figure 1A–F'**, quantified in **Figure 1H**). However, we observed a small decrease in the average number of $Sox2^+$ cells between 6 and 72 hpl, which quickly recovered by 7 dpl (**Figure 1H**). In contrast, we detected an increase in $Sox2^+$ cells at 14 dpl (**Figure 1H**; all groups *versus* 14 dpl: $P < 0.0001$).

The 24 hpl timepoint seemed to be key for regeneration. We observed great variability in the number of $Sox2^+$ cells, and *sox10:tagRFP* oligodendrocytes reached their lowest number. However, from this timepoint onward, we found double-positive cells for *sox10:tagRFP* and Sox2 (*sox10:tagRFP*/$Sox2^+$ cells) at 24 hpl, 72 hpl, 7 dpl and 14 dpl (**Figure 1D–F'**, quantified in **Figure 1I**; control and 6 hpl *versus* 24 hpl: $P < 0.0001$). The highest level of colocalization was found at 24 hpl (**Figure 1I**), which likely reveals that OPCs differentiate into oligodendrocytes *in situ*. We also observed another key colocalization event at 14 dpl (**Figure 1I**; control and 6 hpl *versus* 14 dpl: $P < 0.0001$; 72 hpl *versus* 14 dpl: $P < 0.001$; 7 dpl *versus* 14 dpl: $P < 0.05$). These phenomena might be related to undifferentiated oligodendrocytes that repopulate the ON.

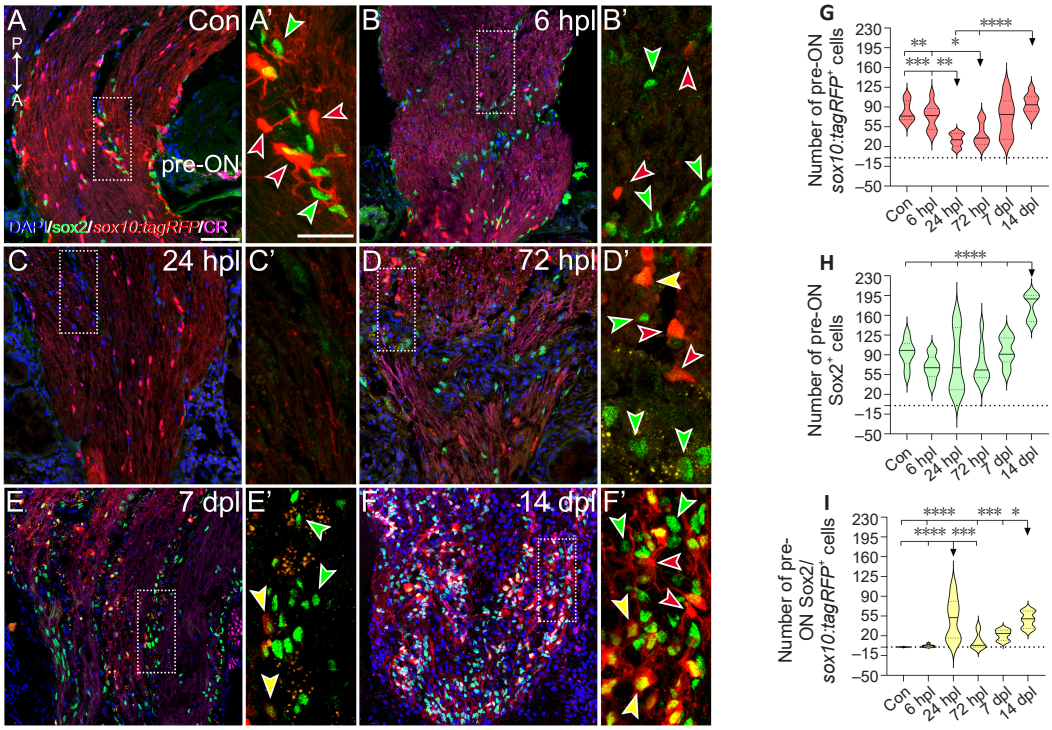

Figure 1 | **Distribution and abundance of *sox10:tagRFP* oligodendrocytes and Sox2-positive cells in the pre-ON of control and injured zebrafish.**
(A–F′) Immunostaining for Sox2-positive cells (green) and axons (CR, magenta) in the ON of a zebrafish transgenic line carrying the *sox10:tagRFP* reporter (red). Nuclei were counterstained with DAPI (blue). Control and inset (A, A'). 6 hpl and inset (B, B'). 24 hpl and inset (C, C'). 72 hpl and inset (D, D'). 7 dpl and inset (E, E'). 14 dpl and inset (F, F'). Red arrows indicate *sox10:tagRFP* oligodendrocytes, green arrows indicate Sox2-positive cells, and yellow arrows indicate double *sox10:tagRFP*/Sox2-positive cells. Scale bar: 50 µm, 25 µm in the inset. The dotted boxes indicate the position of the inset in each group. (G–I) Quantification of the number of *sox10:tagRFP* oligodendrocytes (G), Sox2-positive cells (H), and double *sox10:tagRFP*/Sox2-positive cells in the pre-ON (I). A: Anterior; CR: calretinin; DAPI: 4′,6-diamidino-2-phenylindole; dpl: days post-lesion; hpl: hours post-lesion; P: posterior; pre-ON: prechiasmatic optic nerve. *P < 0.05, **P < 0.01, ***P < 0.001, ****P < 0.0001 (one-way analysis of variance with Tukey's multiple comparison test). The black arrows in the graphs indicate the groups compared. Immunostaining was repeated three times in four different animals from each group.

Thus, our results indicate that *sox10:tagRFP* oligodendrocytes quickly disappear from the point of injury. Then, from 24 hpl onwards Sox2$^+$ stem cells differentiate into new oligodendrocytes.

Fully differentiated oligodendrocytes change their morphology before disappearing

The reduction in *sox10:tagRFP* oligodendrocytes from injured ONs occurred simultaneously with cell morphological changes. *Sox10:tagRFP* oligodendrocytes that remain adjacent to the crush site lose their characteristic shape (**Figure 1B'–E'**), becoming rounded with fewer or no extensions. To further characterize this phenomenon, we quantified the fluorescence intensity of *sox10:tagRFP* oligodendrocytes in the pre-ON area (**Figure 2**). At 6 hpl, in the injured right ON (RON), we observed a reduction in the *sox10:tagRFP* oligodendrocyte fluorescence intensity (**Figure 2B'**, quantified in **Figure 2G**; control *versus* 6 hpl: P < 0.0001). This reduction was maintained at 24 hpl (**Figure 2C'**, quantified in **Figure 2G**; control *versus* 24 hpl: P < 0.0001). By 72 hpl and 7 dpl, the *sox10:tagRFP* oligodendrocyte fluorescence intensity recovered and was closer to that of the control ON (**Figure 2D'** and **E'**; quantified in **Figure 2G**; control *versus* 72 hpl: P < 0.01; control *versus* 72 dpl: P < 0.05). Finally, at 14 dpl, *sox10:tagRFP* oligodendrocyte fluorescence was more intense than that in control fish (**Figure 2F'**, quantified in **Figure 2G**; all groups *versus* 14 dpl: P < 0.0001). We also quantified the *sox10:tagRFP* fluorescence intensity in the left ON (LON) to compare it with that in the injured one (**Figure 2A–F**, quantified in **Figure 2H**, and compared to the RON in **Figure 2I**). We observed no changes in the fluorescence intensity of *sox10:tagRFP* oligodendrocytes in the uninjured ON (**Figure 2H**). The comparison between the oligodendrocytes of the injured and uninjured ON also confirmed the changes these cells underwent (**Figure 2I**; all timepoints except control LON *versus* RON: P < 0.0001). Therefore, ON crush alters the number and distribution of *sox10:tagRFP* oligodendrocytes in pre-ONs very early, but it does not alter the number or distribution of Sox2$^+$ cells until several days later.

Thus, our results indicate that fully differentiated oligodendrocytes (*sox10:tagRFP*) shrink and die. Then, they are replaced by new oligodendrocytes that are produced by resident OPCs (Sox2$^+$ cells).

The stem cells and oligodendrocytes located on both sides of the injury site behave similarly

We wondered if the posterior portion of the ON, the one closer to the optic chiasm (post-ON), behaved similarly to the one closer to the retina. Indeed, we observed similar results with respect to the crushed area, with small differences (**Figure 3**). We also detected an early negative trend in fully differentiated oligodendrocytes (**Figure 3B–D'**, quantified in **Figure 3G**; 24 hpl *versus* 72 hpl: P < 0.05), which recovered by 14 dpl (**Figure 3E–F'**, quantified in **Figure 3G**; 72 hpl *versus* 7 dpl: P < 0.01). We also observed similar changes in the morphology of *sox10:tagRFP* oligodendrocytes, as they were rounder and had fewer or no extensions (**Figure 3B'–C'**). Sox2$^+$ cells were significantly more abundant in post-ONs than in the control at 7 and 14 dpl (**Figure 3B–F'**, quantified in **Figure 3H**; control *versus* 7 dpl to control: P <0.001; control *versus* 14 dpl: P < 0.0001). Finally, the colocalization events in the post-ON group were very similar to those in the pre-ON group, and we detected double *sox10:tagRFP*/Sox2$^+$ cells at 24 hpl, 72 hpl, 7 dpl, and 14 dpl (**Figure 3D'–F'**, quantified in **Figure 3I**, control *versus* 24 hpl, 72 hpl, 7 dpl and 14 dpl: P < 0.05).

Thus, both regions surrounding the crush, the one closer to the retina and the one closer to the optic chiasm, behave similarly.

New *sox10:tagRFP* oligodendrocytes do not seem to originate directly from the retinal peripheral germinal zone

Retinal cells, mainly stem cells, Müller glia, and ganglion cells, also respond to injury (Stella et al., 2021). Thus, we explored whether there were any changes in the *sox10:tagRFP* and Sox2 populations after crush in the retina. Indeed, the stem cells located in the PGZ (Sox2$^+$) quickly proliferate after injury (**Figure 4A–B'**). We observed an important increase in Sox2 staining, which was very evident at 6 hpl (**Figure 4B** and **B'**) and was maintained at least until 72 hpl (**Figure 4C–D'**). During this period, Sox2$^+$ cells also extended further into the

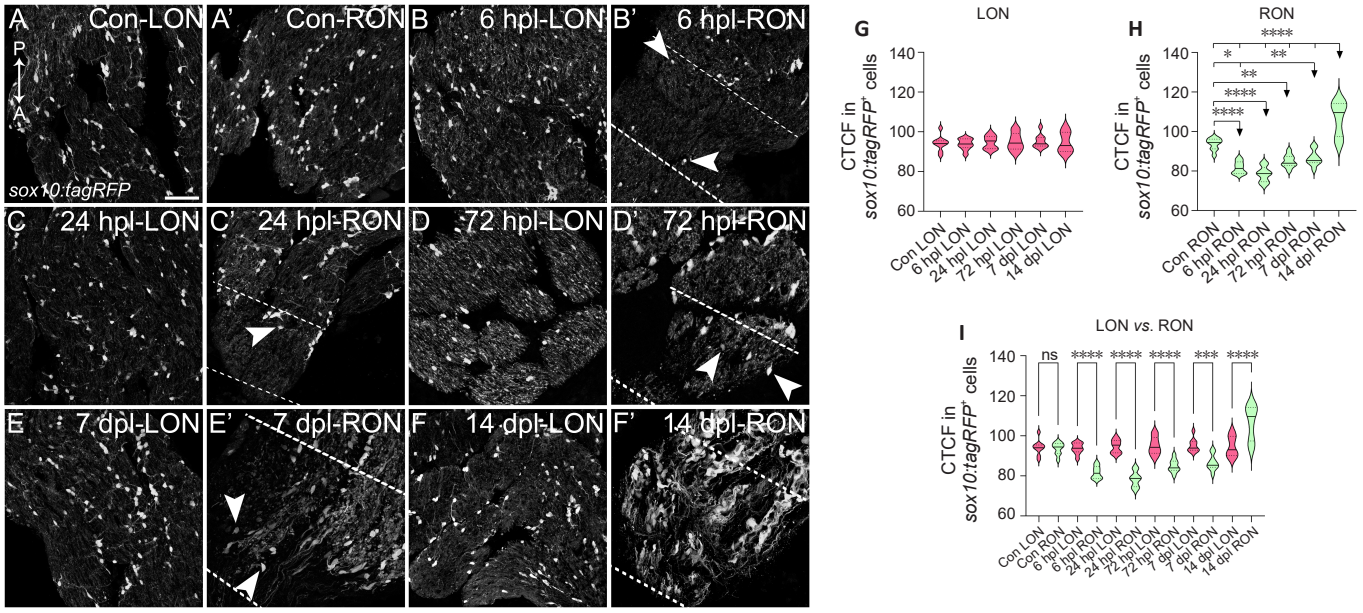

Figure 2 | **Fluorescence intensity of *sox10:tagRFP* in ONs during regeneration.**

(A–F′) Zebrafish transgenic line carrying the *sox10:tagRFP* reporter (gray). Control LON (A) and RON (A′). 6 hpl LON (B) and RON (B′). 24 hpl LON (C) and RON (C′). 72 hpl LON (D) and RON (D′). 7 dpl LON (E) and RON (E′). 14 dpl LON (F) and RON (F′). The white arrows mark *sox10:tagRFP* oligodendrocytes with rounded bodies and few or no extensions. The dashed line marks the crushed zone. Scale bar: 50 µm. The dotted line indicates a crushed ON. (G–I) Fluorescence intensity quantification of *sox10:tagRFP* oligodendrocytes in pre-ON LONs (G) and RON (H) and comparison of LON and RON (I). A: Anterior; dpl: days post-lesion; hpl: hours post-lesion; LON: left optic nerve; P: posterior; RON: right optic nerve. **P* < 0.05, ***P* < 0.01, ****P* < 0.001, *****P* < 0.0001 (one-way analysis of variance with Tukey's multiple comparison test [G and H] and Student's *t* test [I]). The black arrows in the graphs indicate the groups compared. Immunostaining was repeated three times in four different animals from each group.

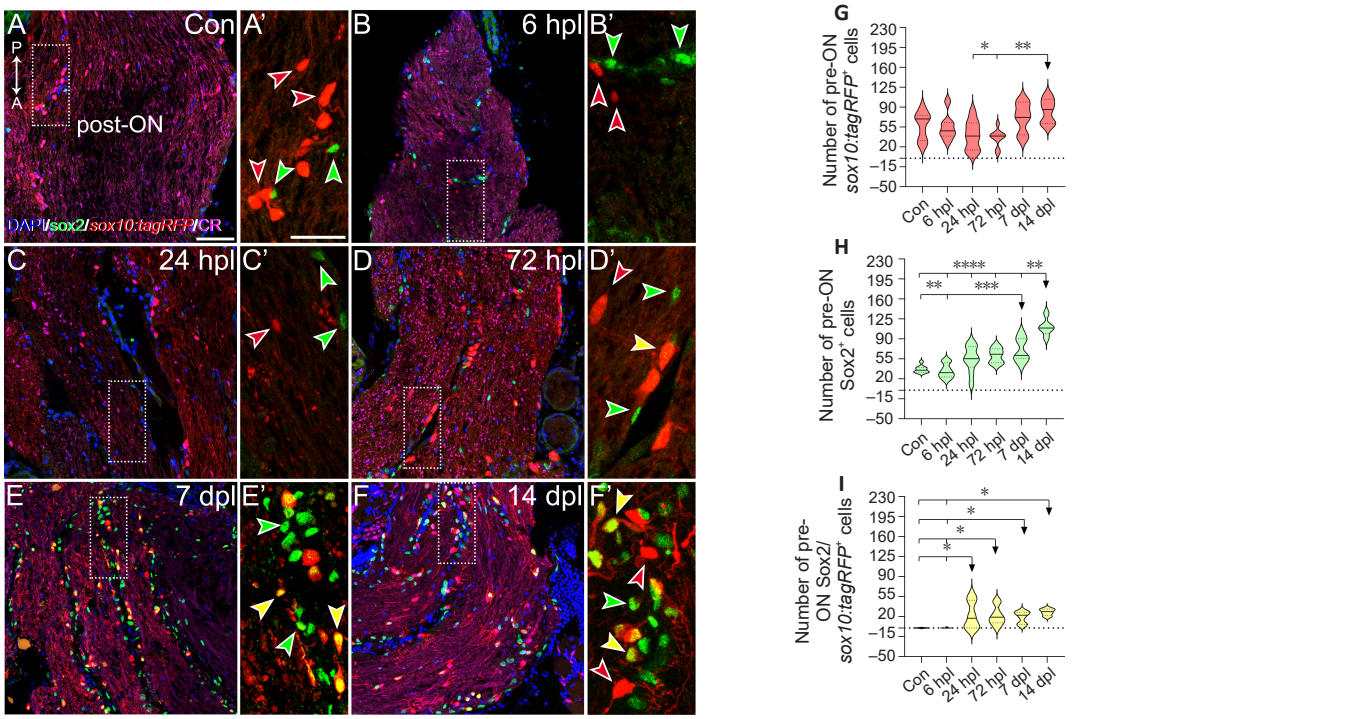

Figure 3 | **Distribution and abundance of *sox10:tagRFP* oligodendrocytes and Sox2-positive cells in post-ON in control and injured zebrafish.**

(A–F′) Immunostaining for Sox2-positive cells (green) and axons (CR, magenta) in the post-ON of a zebrafish transgenic line carrying the *sox10:tagRFP* reporter (red). Nuclei were counterstained with DAPI (blue). Control and inset (A, A′). 6 hpl and inset (B, B′). 24 hpl and inset (C, C′). 72 hpl and inset (D, D′). 7 dpl and inset (E, E′). 14 dpl and inset (F, F′). Red arrows indicate *sox10:tagRFP* oligodendrocytes, green arrows indicate Sox2-positive cells, and yellow arrows indicate double sox10:tagRFP/Sox2-positive cells. Scale bar: 50 µm, 25 µm in the inset. The dotted boxes indicate the position of the inset in each group. (G–I) Quantification of the number of *sox10:tagRFP* oligodendrocytes (G), Sox2-positive cells (H), and double *sox10:tagRFP*/Sox2-positive (I) cells post-ON. A: Anterior; CR: calretinin; dpl: days post-lesion; hpl: hours post-lesion; P: posterior; post-ON: post-chiasmatic optic nerve. **P* < 0.05, ***P* < 0.01, ****P* < 0.001, *****P* < 0.0001 (one-way analysis of variance with Tukey's multiple comparison test). The black arrows in the graphs indicate the groups compared. Immunostaining was repeated three times in four different animals from each group.

mature retina (**Figure 4B'**). By 7 dpl, Sox2 staining in the PGZ decreased and was very close to that of the controls (**Figure 4E** and **E'**), and no differences were observed at 14 dpl (**Figure 4F** and **F'**), which is usually considered full recovery (Stella et al., 2021). We did not observe any fully differentiated oligodendrocytes (*sox10:tagRFP*) in the PGZ or close to it, and there were no changes during regeneration (**Figure 4A–F**). Thus, the newly formed oligodendrocytes necessary for regeneration did not arise directly from the PGZ.

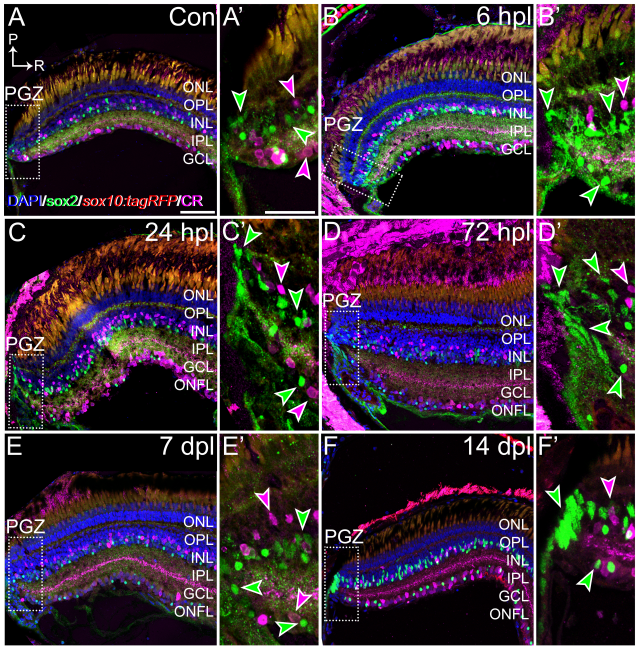

Figure 4 | **Distribution and abundance of *sox10:tagRFP* oligodendrocytes and Sox2-positive cells in the PGZ in control and injured zebrafish.**
(A–F') Immunostaining for Sox2-positive cells (green) and axons (CR, magenta) in the PGZ of a zebrafish transgenic line carrying the *sox10:tagRFP* reporter (red). Nuclei were counterstained with DAPI (blue). Control and inset (A, A'). 6 hpl and inset (B, B'). 24 hpl and inset (C, C'). 72 hpl and inset (D, D'). 7 dpl and inset (E, E'). 14 dpl and inset (F, F'). The green arrows indicate Sox2-positive cells, and the magenta arrows indicate CR-positive cells. CR: Calretinin; dpl: days post-lesion; GCL: ganglion cell layer; hpl: hours post-lesion; INL: inner nuclear layer; IPL: inner plexiform layer; ONFL: optic nerve fiber layer; ONL: outer nuclear layer; OPL: outer plexiform layer; P: posterior; PGZ: peripheral germinal zone; R: right. Scale bar: 50 µm, 25 µm in the inset. The dotted boxes indicate the position of the inset in each group. Immunostaining was repeated three times in four different animals from each group.

Sox2$^+$ stem cells and *Sox10:tagRFP* oligodendrocytes are located in the INL, and the optic nerve fiber layer responds to optic nerve crush

Our preliminary analysis revealed the presence of *sox10:tagRFP* cells in other retinal layers. Therefore, we wondered whether these cells also respond to ON damage. In the central retina (**Figure 5**), *sox10:tagRFP* oligodendrocytes were present in the GCL and extended into the ONFL (**Figure 5A** and **A'**). Most of the Sox2$^+$ cells were found in the INL and in the GCL, some were in the IPL, and the ONFL presented the fewest (**Figure 5A** and **A'**). Thus, *sox10:tagRFP* oligodendrocytes and Sox2$^+$ cells coexisted in the GCL and, mostly, in the ONFL. However, we did not find any colocalization between these markers in control animals (**Figure 5A'**, quantified in **K**). After ON crush, we did not observe any changes in the location of these cells, but we observed an increase in the number of both types of cells and, also, in the colocalization of the markers (**Figure 5B–F'**, quantified in **Figure 5G–K**).

We found approximately 9 *sox10:tagRFP* oligodendrocytes per analyzed area distributed in the GCL and the ONFL (**Figure 5A** and **A'**, quantified in **Figure 5G**). We observed a slight but steady increase that peaked at 72 hpl, with 16 *sox10:tagRFP* oligodendrocytes per analyzed area (**Figure 5D** and **D'**, quantified in **Figure 5G**). By 7 dpl, the number of *sox10:tagRFP* oligodendrocytes was still high and similar to that at 72 hpl (**Figure 5E**, **E'**, quantified in **Figure 5G**; control *versus* 7 dpl: $P < 0.01$). Finally, at 14 dpl, we observed a further increase in the number of 21 *sox10:tagRFP* oligodendrocytes per section (**Figure 5F** and **F'**, quantified in **Figure 5G**; control *versus* 14 dpl: $P < 0.0001$). The number of Sox2$^+$ cells also gradually increased throughout the time points studied in the INL (**Figure 5A–F**, quantified in **Figure 5H**), and their number at 7 dpl was the highest (**Figure 5E** and **E'**, quantified in **Figure 5H**; control *versus* 7 dpl: $P < 0.0001$; 6 hpl, 24 hpl and 27 hpl *versus* 7 dpl: $P < 0.01$; 14 dpl *versus* 7 dpl: $P < 0.05$). Although we observed some changes in the population of Sox2$^+$ cells in the GCL and the ONFL, the variation was not significant, except in the ONFL at 14 dpl (**Figure 5B–F**, quantified in **Figure 5I** and **J**; all groups *versus* 14 dpl: $P < 0.0001$).

Interestingly, we found double *sox10:tagRFP*/Sox2$^+$ cells in the ONFL at 7 dpl and 14 dpl (**Figure 5E–F'**, quantified in **Figure 5K**; control, 6 hpl, 24 hpl and 72 hpl *versus* 7 dpl: $P < 0.0001$; control, 6 hpl, 24 hpl and 72 hpl *versus* 14 dpl: $P < 0.0001$), which occurred later than in the ON (**Figure 1**). We could not find any other colocalization events in any other layer or at any of the other time points studied. These findings suggest that, under regenerative conditions, some Sox2$^+$ OPCs in the ONFL are capable of differentiating into oligodendrocytes in the area where the ON starts.

Our results indicate that, in response to damage, Sox2$^+$ stem cells located in the ONFL differentiate into oligodendrocytes at 7 dpl, a little bit later than in the ON.

Sox2$^+$ stem cells continue their differentiation into *sox10:tagRFP* oligodendrocytes along the optic nerve head

In the ONH, as in the mature retina, the number of *sox10:tagRFP* oligodendrocytes and Sox2$^+$ cells increased after ON crush, but this change was observed earlier (**Figure 6A–F**, quantified in **Figure 6G** and **H**). The number of *sox10:tagRFP* oligodendrocytes in the ONH was similar to that in the control fish along the study but increased gradually (**Figure 6A–F**, quantified in **Figure 6G**). At 7 dpl, we observed many *sox10:tagRFP* oligodendrocytes (**Figure 6E** and **E'**, quantified in **Figure 6G**; control and 6 hpl *versus* 7 dpl: $P < 0.0001$). At 14 dpl, the number of *sox10:tagRFP* oligodendrocytes decreased, recovering to normal levels (**Figure 6F** and **F'**, quantified in **Figure 6G**; 14 dpl *versus* 7 dpl: $P < 0.0001$). At 6 hpl, Sox2$^+$ cells were slightly more abundant in the regenerated fish than in the control fish, but this difference was not significant (**Figure 6B** and **B'**, quantified in **Figure 6H**). From that timepoint, the number of Sox2$^+$ cells increased and peaked at 7 dpl (**Figure 6E** and **E'**, quantified in **Figure 6H**; control *versus* 7 dpl: $P < 0.0001$; 6 hpl *versus* 7 dpl: $P < 0.001$), which was consistent with the peak of *sox10:tagRFP* oligodendrocytes. This increase was maintained at 14 dpl (**Figure 6F** and **F'**, quantified in **Figure 6H**; control, 6 hpl, and 24 hpl *versus* 14 dpl: $P < 0.0001$; 72 hpl *versus* 14 dpl: $P < 0.001$; 7 dpl *versus* 14 dpl: $P < 0.05$). Interestingly, we found double *sox10:tagRFP*/Sox2$^+$ cells at 7 dpl and 14 dpl, as we did in the central retina (**Figure 6E–F'**, quantified in **Figure 6I**; control, 6 hpl, 24 hpl and 72 hpl *versus* 7 dpl: $P < 0.01$; control, 6 hpl and 24 hpl *versus* 14 dpl: $P < 0.0001$; 72 hpl *versus* 14 dpl: $P < 0.001$).

Thus, a second differentiation event seems to have occurred in the ONFL and the ONH. These myelinating oligodendrocytes leave the retina through the ONH toward the injury site as the axons regenerate.

Death and proliferation after optic nerve crush

We reported that, after ON crush, there was a decrease in the number of *sox10:tagRFP* oligodendrocytes in the injured ON area, together with a loss of their characteristic morphology (cells with large soma and many extensions), resulting in round cells with few or no extensions (**Figures 1** and **2**). We wondered whether this reduction in the crushed area was due to cell death after ON degeneration. To test this hypothesis, we used the click-iT^{TM} Plus TUNEL Assay Kit, which detects apoptotic cells in tissues *in situ* (**Figure 7A–E'**, quantified in **F** and **G**). We analyzed both ONs, the injured right ON (RON) and the uninjured left ON (LON). We found more apoptotic cells at 6 hpl in the RON (**Figure 7B'**, quantified in **Figure 7F**, and compared with LON in **Figure 7G**; control *versus* 6 hpl: $P < 0.01$; LON *versus* RON at 6 hpl: $P < 0.01$). However, these TUNEL-positive cells were negative for *sox10:tagRFP*, indicating that oligodendrocytes do not disappear by apoptosis and are positive for TUNEL.

After ON crush, *sox10:tagRFP* cells recovered from 72 hpl, and the Sox2$^+$ cell number was maintained in the injured ON area until 14 dpl (**Figure 1**). We also described the presence of double *sox10:tagRFP*/Sox2$^+$ cells at 24 hpl, 72 hpl, 7 dpl, and 14 dpl. We performed an assay with BrdU, which allows an almost total substitution (99.8%–100%) of the thymidine nucleotides in cells in the S phase of the cell cycle. For this experiment (**Figure 7H**), we used control fish and 72 hpl fish, since we observed a recovery in the number of *sox10:tagRFP* oligodendrocytes in the injured ON during this time. Therefore, 24 hours before 72 hours after injury, we administered a fresh solution of 5 mM BrdU diluted in the tank. At the same time, control fish were administered a fresh solution of 5 mM BrdU diluted in tank water for 24 hours (**Figure 7H**). The control fish presented some proliferating cells, both in the RON and the LON (**Figure 7J**, quantified in **Figure 7I**). At 72 hpl, we observed many proliferating cells, especially in the crushed ON area and in the ON-injured area itself (**Figure 7K**, quantified in **Figure 7I**; LON *versus* RON: $P < 0.0001$). These BrdU$^+$ cells were not positive for *sox10:tagRFP*. Thus, the oligodendrocytes that remain after injury do not give rise to more oligodendrocytes. The newly incorporated cells detected from 72 hpl onward are probably formed by the double *sox10:tagRFP*/Sox2$^+$ we identified first in the injured area (**Figure 1**) and later in the retina (**Figure 5** and **6**).

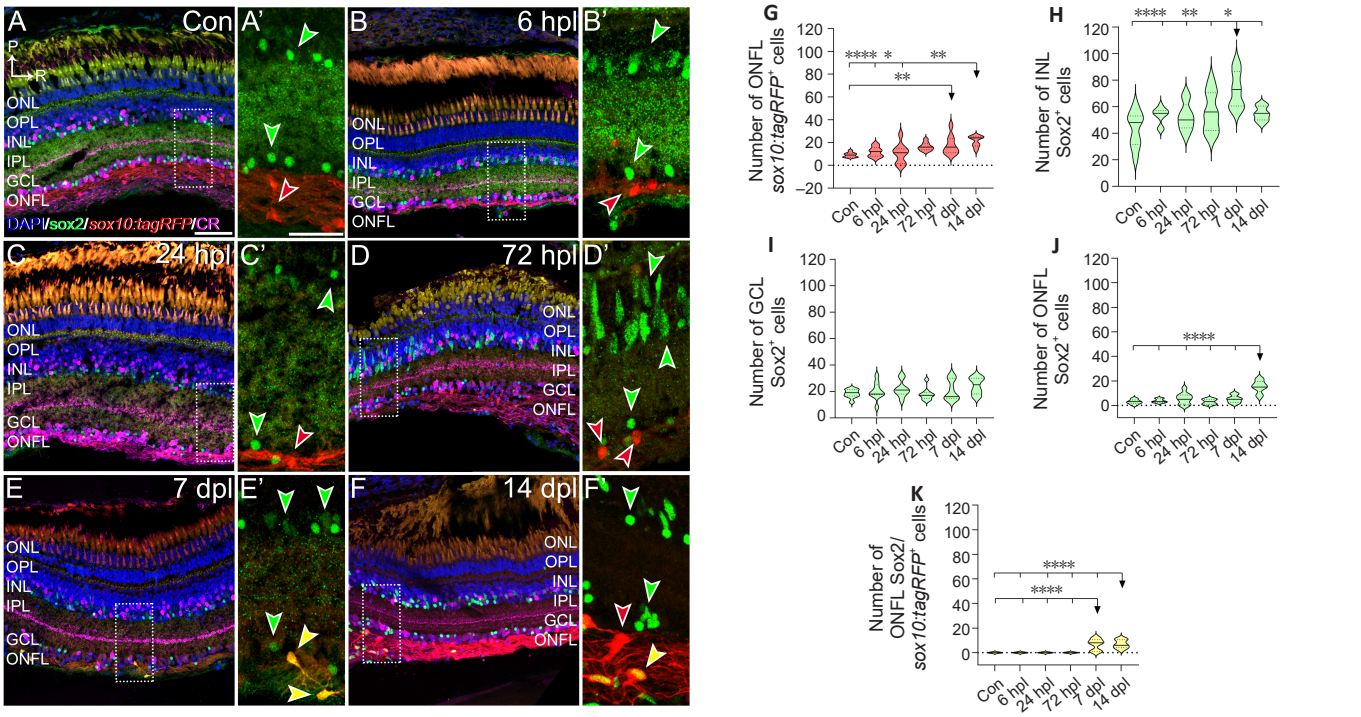

Figure 5 | **Distribution and abundance of *sox10:tagRFP* oligodendrocytes and Sox2-positive cells in the central retina of control and injured zebrafish.**
(A–F') Immunostaining for Sox2-positive cells (green) and axons (CR, magenta) in the central retina of a zebrafish transgenic line carrying the *sox10:tagRFP* reporter (red). Nuclei were counterstained with DAPI (blue). Control and inset (A, A'). 6 hpl and inset (B, B'). 24 hpl and inset (C, C'). 72 hpl and inset (D, D'). 7 dpl and inset (E, E'). 14 dpl and inset (F, F'). Red arrows indicate *sox10:tagRFP* oligodendrocytes, green arrows indicate Sox2-positive cells, and yellow arrows indicate double *sox10:tagRFP*/Sox2-positive cells. Scale bar: 50 μm, 25 μm in the inset. The dotted boxes indicate the position of the inset in each group. (G–K) Quantification of the following numbers of cells: *sox10:tagRFP* oligodendrocytes (G), Sox2-positive cells in the INL (H), Sox2-positive cells in the GCL (I), Sox2-positive cells in the OFL (J), and double *sox10:tagRFP*/Sox2-positive cells in the ONFL (K). CR: Calretinin; dpl: days post-lesion; GCL: ganglion cell layer; hpl: hours post-lesion; INL: inner nuclear layer; IPL: inner plexiform layer; ONFL: optic nerve fiber layer; ONL: outer nuclear layer; OPL: outer plexiform layer; P: posterior; PGZ: peripheral germinal zone; R: right. **P* < 0.05, ***P* < 0.01, *****P* < 0.0001 (one-way analysis of variance with Tukey's multiple comparison test). The black arrows in the graphs indicate the groups compared. Immunostaining was repeated three times in four different animals from each group.

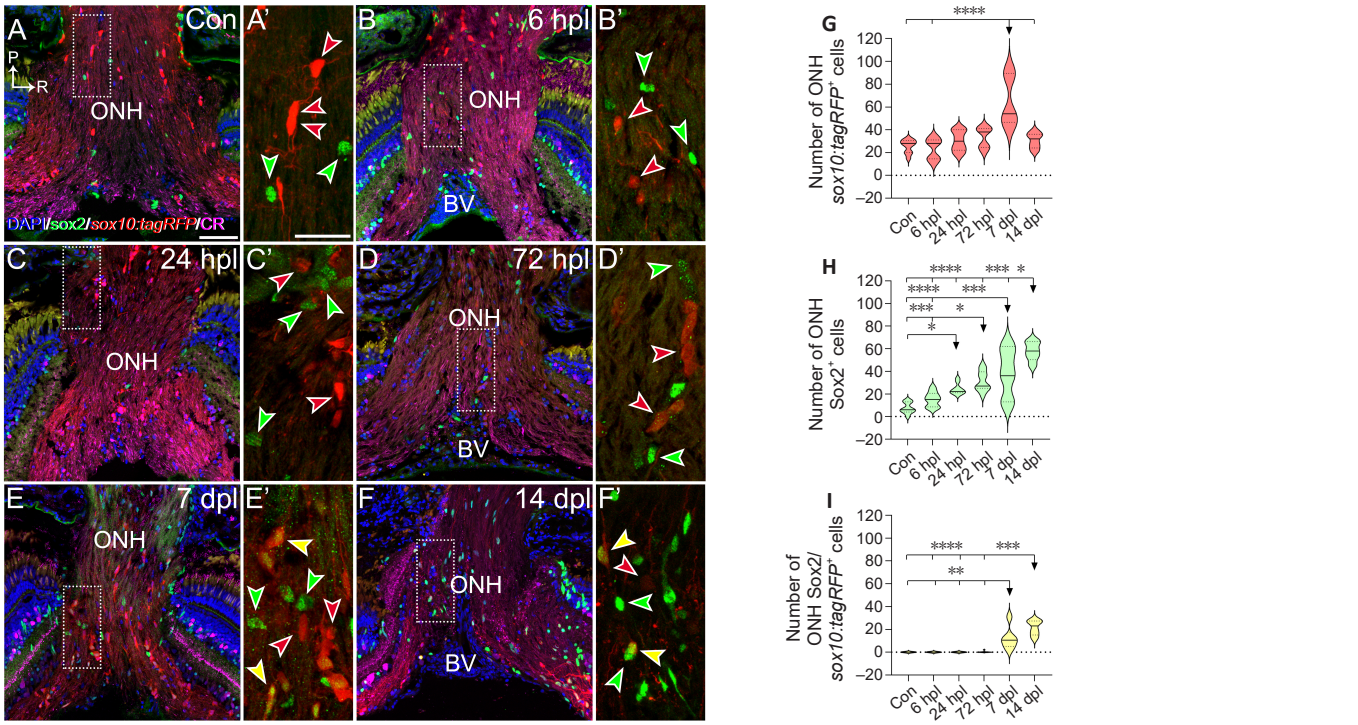

Figure 6 | **Distribution and abundance of *sox10:tagRFP* oligodendrocytes and Sox2-positive cells in the ONH of control and injured zebrafish.**
(A–F') Immunostaining for Sox2-positive cells (green) and axons (CR, magenta) in the ONH of a zebrafish transgenic line carrying the *sox10:tagRFP* reporter (red). Nuclei were counterstained with DAPI (blue). Control and inset (A, A'). 6 hpl and inset (B, B'). 24 hpl and inset (C, C'). 72 hpl and inset (D, D'). 7 dpl and inset (E, E'). 14 dpl and inset (F, F'). Red arrows indicate *sox10:tagRFP* oligodendrocytes, green arrows indicate Sox2-positive cells, and yellow arrows indicate double *sox10:tagRFP*/Sox2-positive cells. Scale bar: 50 μm, 25 μm in the inset. The dotted boxes indicate the position of the inset in each group. (G–I) Quantification of the number of *sox10:tagRFP* oligodendrocytes (G), Sox2-positive cells (H) and double *sox10:tagRFP*/Sox2-positive cells (I) in the ONH. BV: Blood vessel; CR: calretinin; dpl: days post-lesion; hpl: hours post-lesion; ONH: optic nerve head; P: posterior; R: right. **P* < 0.05, ***P* < 0.01, ****P* < 0.001, *****P* < 0.0001 (one-way analysis of variance with Tukey's multiple comparison test). The black arrows in the graphs indicate the groups compared. Immunostaining was repeated three times in four different animals from each group.

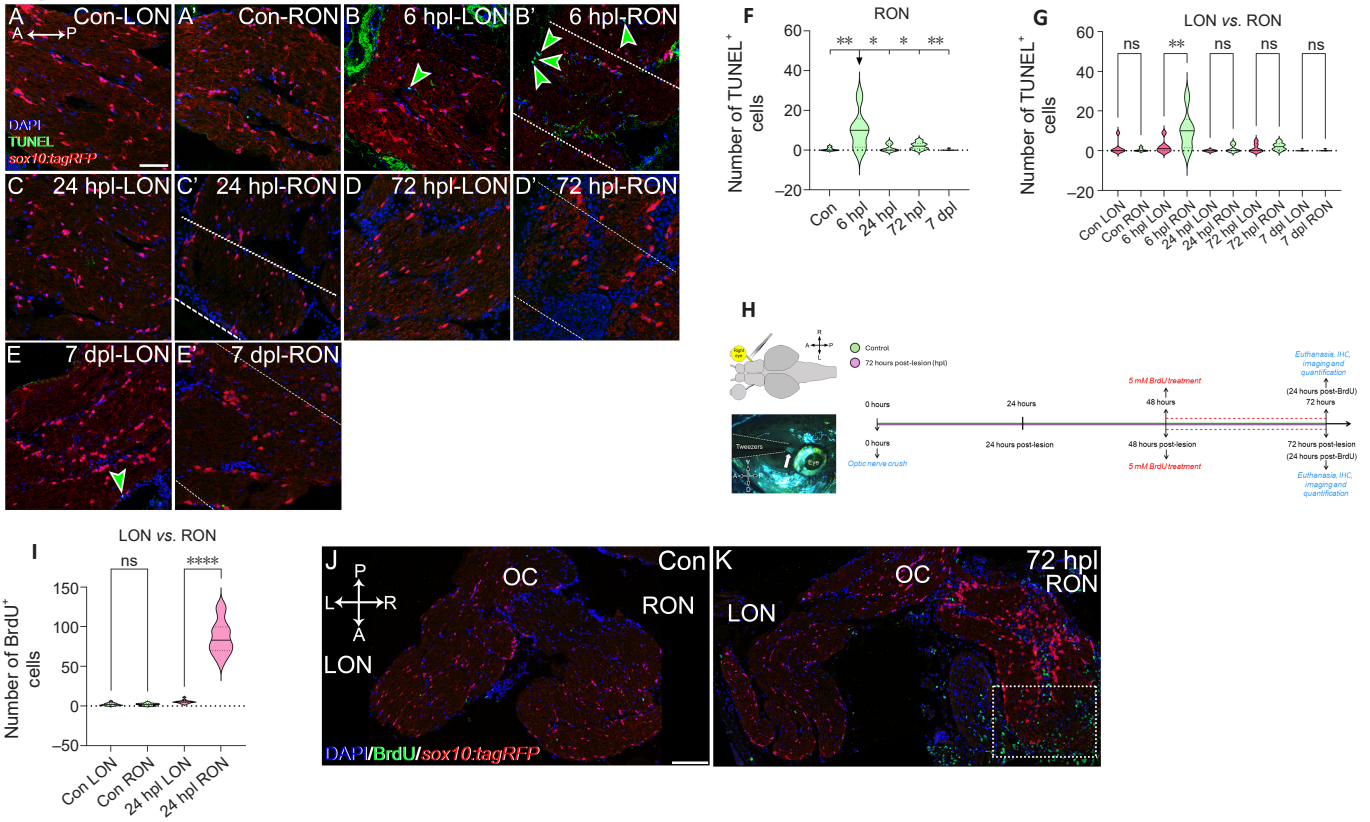

Figure 7 | **Distribution and abundance of TUNEL-positive cells and BrdU-positive cells in both ONs of control and regenerating zebrafish.**
(A–E') Immunostaining for TUNEL-positive cells (green) in the ONs of a zebrafish transgenic line carrying the *sox10:tagRFP* reporter (red). Nuclei were counterstained with DAPI (blue). Control LON (A) and RON (A'). 6 hpl LON and RON (B'). 24 hpl LON (C) and RON (C'). 72 hpl LON (D) and RON (D'). 7 dpl LON (E) and RON (E'). The green arrows indicate TUNEL-positive cells. The dashed line marks the crushed zone. (F, G) Quantification of TUNEL-positive cells in the RON (F) and comparison of RON and LON (G) groups. (H) Schematic representation of the BrdU assay. (I) Quantification of BrdU-positive cells in the LON compared with the RON. (J, K) Immunostaining for BrdU-positive cells (green) in the ONs of a zebrafish transgenic line carrying the *sox10:tagRFP* reporter (red). The white rectangle indicates the crushed zone. The control fish were exposed to BrdU for 24 hours (J). 72 hpl fish exposed for 24 hours to BrdU (K). A: anterior; dpl: days post-lesion; hpl: hours post-lesion; L: left; LON: left optic nerve; OC: optic chiasm; P: posterior; R: right; RON: right optic nerve. $*P < 0.05$, $**P < 0.01$, $****P < 0.0001$ (one-way analysis of variance with Tukey's multiple comparison test [F] and Student's *t* test [G and I]). The black arrows in the graphs indicate the groups compared. Scale bars: 50 µm (A-E'), 100 µm (J and K). The dotted boxes and lines indicate the crushed ON. Immunostaining was repeated three times in four different animals from each group.

Thus, damaged *sox10:tagRFP* oligodendrocytes die via a mechanism other than typical apoptosis, and new ones arise from Sox2$^+$ stem cells

Discussion

Sox10 is a highly conserved transcription factor with similar roles in fish, mice, and humans (Wegner and Stolt, 2005; Pingault et al., 2022). Sox10 is necessary for the specification of the oligodendrocyte lineage and their survival during differentiation (Wegner and Stolt, 2005; Wegner, 2008). It contributes to the maturation of OPCs to mature, myelinating oligodendrocytes (Takada and Appel, 2010; Santos-Ledo et al., 2023). Sox10 induces the expression of some myelin genes, such as myelin basic protein (MBP) (Boggs, 2006), and indirectly mediates oligodendrocyte–axon interactions (Takada and Appel, 2010). In the adult CNS, the functions of Sox10 are less explored, but Sox10 is present in mature oligodendrocytes, maintaining their oligodendroglial phenotype (Parrilla et al., 2016).

In this work, we used the transgenic line *sox10:tagRFP* (Blasky et al., 2014) to track fully differentiated oligodendrocytes in the visual system of adult zebrafish before and during regeneration (6, 24 and 72 hpl; 7 and 14 dpl), together with Sox2 immunohistochemistry, a stem cell marker, to understand the changes that these oligodendrocytes undergo during regeneration. We show that before ON crush, *sox10:tagRFP* oligodendrocytes are distributed in groups and rows in all visual areas, as previously described in other fish (Münzel et al., 2014; Parrilla et al., 2016). Intraretinal oligodendrocytes have been described in other animals, such as birds (Won et al., 2000), reptiles (Fujita et al., 2000) and amphibians (Kalinina, 1983), which are believed to be involved in myelination, nutrition, and maintenance of ganglion cells (Won et al., 2000; Santos et al., 2006). The fish retina is not myelinated, and oligodendrocytes maintain some immature characteristics due to environmental factors (Münzel et al., 2012). Sox2 cells are present in the immature and mature retina (PGZ and central retina) and throughout the entire length of the ON, whereas the ONH is almost devoid of these cells, as has been previously described (Gorsuch et al., 2017; DeOliveira-Mello et al., 2019). Interestingly, in the anterior portion of the ON, the ONH–ON transition zone, Sox2$^+$ cells are distributed next to *sox10:tagRFP* oligodendrocytes. This finding suggests a role in the organization of the newly formed axons (DeOliveira-Mello et al., 2019).

After ON crush, the number of *sox10:tagRFP* oligodendrocytes decreases in the injured ON area, as occurs in mice (Ghaddar et al., 2021). This death seems to be a requirement for efficient regeneration (Neely et al., 2022). They also lose their characteristic morphology (large soma and many extensions), becoming round with few or no extensions. Oligodendrocytes are extremely vulnerable to damage due to their susceptibility to oxidative stress (Thorburne and Juurlink, 1996; Dent et al., 2015). The high energy demand required for myelin production leads to the accumulation of toxic metabolites and reactive oxygen species (Pérez-Montes et al., 2023). Thus, situations related to high metabolic or oxidative stress are likely to overload these cells and result in cell death. However, our results indicate that there are no TUNEL-positive cells, and it seems unlikely that these cells die via standard apoptosis. Other types of cell death must be considered. For example, autophagy can trigger cell death to control the number of oligodendrocytes during development (Zhang et al., 2023a). Autophagy maintains cellular homeostasis and recycles cytoplasmic contents, and emerging evidence suggests that autophagy is a primary mechanism of cell death (Jung et al., 2020). It would be interesting to investigate whether this is also true during zebrafish ON regeneration.

At 72 hpl, the number of *sox10:tagRFP* oligodendrocytes in the pre-ON started to recover. This occurred simultaneously with the appearance of double

sox10:tagRFP/Sox2$^+$ cells in the injured ON. OPCs, which are characterized by transcription factors such as Sox2 and Sox10, produce oligodendrocytes (Park et al., 2002; Takada and Appel, 2010; Bhattarai et al., 2022; Santos-Ledo et al., 2023). OPCs rapidly migrate and ensheathe axons, where they differentiate into myelinating oligodendrocytes (Nawaz et al., 2013; Münzel et al., 2014). During zebrafish CNS development, OPCs express Sox2, and they switch to Sox10 as they differentiate (Santos-Ledo et al., 2023; Rupprecht et al., 2024). In response to oligodendrocyte damage, residual OPCs initiate their proliferation and differentiation, a process partially supported by neighboring cells (Ohtomo et al., 2018). Axon-secreted molecules or axonal surface ligands also contribute to this process (Ohtomo and Arai, 2020). Therefore, the appearance of *sox10:tagRFP*/Sox2$^+$ cells in the injured ON might be a consequence of the differentiation of OPCs to mature oligodendrocytes. This hypothesis is reinforced by the lack of BrdU in fully differentiated oligodendrocytes but by the existence of many proliferating cells in the area. Therefore, these double *sox10:tagRFP*/Sox2$^+$ cells detected at 72 hpl may be derived from the Sox2 resident ON cells.

We also detected double-positive *sox10:tagRFP*/Sox2$^+$ cells in the ONH and ONFL of the retina seven days after lesion induction, together with a gradual increase in Sox2$^+$ cells in the INL, ONFL and ONH. Fourteen days after lesion induction, colocalization events were more evident in the ONH. These Sox2$^+$ cells could be glial precursors necessary to receive, guide, support, orient and myelinate new axons (Parrilla et al., 2009; Xiao et al., 2022). After ON crush, these precursors respond and differentiate into oligodendrocytes as they leave the retina toward the injury site. This reaction has been described for Müller glia, another cell type positive for Sox2 located in the INL, where we have also observed a response. Owing to their stem properties, Müller cells are key to maintaining the structural and functional stability of retinal cells and can generate new cells during continuous growth and regeneration in zebrafish (Gorsuch et al., 2017; Lust and Wittbrodt, 2018).

The response and behavior of oligodendrocytes during ON regeneration reveal their plasticity, which is necessary for the full restoration of the injured visual system. Our results indicate that, during degeneration, oligodendrocytes change their morphology, turning rounder, losing projections and, finally, disappearing from the injury site, as indicated in other models (Parrilla et al., 2016). After ON crush, we observed two different events of oligodendrocyte repopulation. The first one was early, at 72 hpl, likely from the Sox2$^+$ cells that reside within the ON together with fully differentiated oligodendrocytes. The second event, a few days later, starts at 7 dpl and begins with the residual Sox2$^+$ OPC cells within the retina. A similar differentiation mechanism has been described in the peripheral nervous system (Zhou et al., 2023). The events described here seem to be necessary for proper regeneration, and newborn oligodendrocytes are key during zebrafish axon regeneration and remyelination.

Limitations

Here, we explored the dynamics of fully differentiated oligodendrocytes via a transgenic line (*sox10:tagRFP*) and the response of stem cells in the visual system (Sox2$^+$ cells). The contributions of other glial cells, such as astrocytes and microglia, which are also important for regeneration, have not been explored. It would be interesting to understand the behavior of all glial cells. We have not yet been able to pinpoint the mechanism of oligodendrocyte death. In the future, it would be very valuable to determine whether the disappearance of oligodendrocytes is mediated by other types of cell death, such as ferroptosis, or by autophagy due to lipid toxicity that may result from degenerative axons.

Conclusions

Nerve crush triggers a decrease in *sox10:tagRFP* oligodendrocytes in the ON together with an increase in Sox2$^+$ cells in the ON, ONH, and retina. Then, between 24 hpl and 14 dpl, double *sox10:tagRFP*/Sox2$^+$ cells were detected in the retina, ONH, and whole ON. We observed two different waves of *sox10:tagRFP* oligodendrocyte differentiation. The first one, early at 24 hpl, is within the ON owing to resident Sox2$^+$ OPCs. The second one, which occurs at 7 dpl, involves the incorporation of Sox2$^+$ stem cells from the retina as new axons grow. One key difference between regeneration in the visual system of zebrafish and mammals is that in the former, damaged oligodendrocytes die and are replaced by new oligodendrocytes. However, in mammals, oligodendrocytes persist and contribute to the glial scar, which is difficult to regenerate. In the future, understanding the exact mechanism of this death and renewal might help to establish more efficient therapies that promote regeneration.

Acknowledgments: *We would like to thank Mª Teresa Sánchez Montero for her technical support. We are members of Women in Autophagy (WIA), Sociedad Española de Bioquímica y Biología Molecular (SEBBM) and Sociedad Española de Autofagia (SEFAGIA).*

Author contributions: *Conceptualization: CPM, LDM, MGM, ASL, and RA. Methodology: CPM, LDM, JPJC, RHG, MGM, and ASL. Formal analysis: CPM, RHG, MGM, and ASL. Original draft: CPM, MGM, ASL and RA. Review and editing: CPM, LDM, AV, MGM, ASL, and RA. All authors read and agreed to this paper.*

Conflicts of interest: *The authors declare that they have no competing interests.*

Data availability statement: *All relevant data are within the paper and its Additional files.*

Additional file:

Additional Figure 1: *Distribution of sox10:tagRFP oligodendrocytes and Sox2-positive cells in the zebrafish visual system.*

References

Ávila-Mendoza J, Urban-Sosa VA, Lazcano I, Orozco A, Luna M, Martínez-Moreno CG, Arámburo C (2024) Comparative analysis of Krüppel-like factors expression in the retinas of zebrafish and mice during development and after injury. Gen Comp Endocrinol 356:114579.

Beccari S, et al. (2023) Microglial phagocytosis dysfunction in stroke is driven by energy depletion and induction of autophagy. Autophagy 19:1952-1981.

Bejarano-Escobar R, Blasco M, Martín-Partido G, Francisco-Morcillo J (2014) Molecular characterization of cell types in the developing, mature, and regenerating fish retina. Rev Fish Biol Fisheries 24:127-158.

Bhattarai C, Poudel PP, Ghosh A, Kalthur SG (2022) Comparative role of SOX10 gene in the gliogenesis of central, peripheral, and enteric nervous systems. Differentiation 128:13-25.

Blasky AJ, Pan L, Moens CB, Appel B (2014) Pard3 regulates contact between neural crest cells and the timing of Schwann cell differentiation but is not essential for neural crest migration or myelination. Dev Dyn 243:1511-1523.

Boggs JM (2006) Myelin basic protein: a multifunctional protein. Cell Mol Life Sci 63:1945-1961.

Breinbauer R, Köhn M (2003) Azide-alkyne coupling: a powerful reaction for bioconjugate chemistry. Chembiochem 4:1147-1149.

Cameron EG, Xia X, Galvao J, Ashouri M, Kapiloff MS, Goldberg JL (2020) Optic nerve crush in mice to study retinal ganglion cell survival and regeneration. Bio Protoc 10:e3559.

Dent KA, Christie KJ, Bye N, Basrai HS, Turbic A, Habgood M, Cate HS, Turnley AM (2015) Oligodendrocyte birth and death following traumatic brain injury in adult mice. PLoS One 10:e0121541.

DeOliveira-Mello L, Lara JM, Arevalo R, Velasco A, Mack AF (2019) Sox2 expression in the visual system of two teleost species. Brain Res 1722:146350.

Fujita Y, Imagawa T, Uehara M (2000) Comparative study of the lamina cribrosa and the pial septa in the vertebrate optic nerve and their relationship to the myelinated axons. Tissue Cell 32:293-301.

Garcia-Pradas L, Gleiser C, Wizenmann A, Wolburg H, Mack AF (2018) Glial cells in the fish retinal nerve fiber layer form tight junctions, separating and surrounding axons. Front Mol Neurosci 11:367.

Ghaddar B, Lübke L, Couret D, Rastegar S, Diotel N (2021) Cellular mechanisms participating in brain repair of adultzebrafish and mammals after injury. Cells 10:1-24.

Gorsuch RA, Lahne M, Yarka CE, Petravick ME, Li J, Hyde DR (2017) Sox2 regulates Müller glia reprogramming and proliferation in the regenerating zebrafish retina via Lin28 and Ascl1a. Exp Eye Res 161:174-192.

Hines JH (2021) Evolutionary origins of the oligodendrocyte cell type and adaptive myelination. Front Neurosci 15:1569.

Hu H, Pang Y, Luo H, Tong B, Wang F, Song Y, Ying Q, Xu K, Xiong C, Peng Z, Xu H, Zhang X (2024) Noninvasive light flicker stimulation promotes optic nerve regeneration by activating microglia and enhancing neural plasticity in zebrafish. Invest Ophthalmol Vis Sci 65:3.

Jung S, Jeong H, Yu SW (2020) Autophagy as a decisive process for cell death. Exp Mol Med 52:921-930.
Kalinina AV (1983) Glial cells of the retina in rana ridibunda pall. Arkh Anat Gistol Embriol 84:33-38.
Liu Q, Londraville RL (2003) Using the adult zebrafish visual system to study cadherin-2 expression during central nervous system regeneration. Methods Cell Sci 25:71-78.
Liu X, Feng L, Shinde I, Cole JD, Troy JB, Saggere L (2020) Correlation between retinal ganglion cell loss and nerve crush force-impulse established with instrumented tweezers in mice. Neurol Res 42:379-386.
Lust K, Wittbrodt J (2018) Activating the regenerative potential of Müller glia cells in a regeneration-deficient retina. Elife 7:1-23.
Masson MA, Nait-Oumesmar B (2023) Emerging concepts in oligodendrocyte and myelin formation, inputs from the zebrafish model. Glia 71:1147-1163.
McDowell AL, Dixon LJ, Houchins JD, Bilotta J (2004) Visual processing of the zebrafish optic tectum before and after optic nerve damage. Vis Neurosci 21:97-106.
Mercurio S, Serra L, Nicolis SK (2019) More than just stem cells: Functional roles of the transcription factor Sox2 in differentiated glia and neurons. Int J Mol Sci 20:4540.
Mercurio S, Alberti C, Serra L, Meneghini S, Berico P, Bertolini J, Becchetti A, Nicolis SK (2021) An early Sox2-dependent gene expression programme required for hippocampal dentate gyrus development. Open Biol 11:200339.
Münzel EJ, Schaefer K, Obirei B, Kremmer E, Burton EA, Kuscha V, Becker CG, Brösamle C, Williams A, Becker T (2012) Claudin k is specifically expressed in cells that form myelin during development of the nervous system and regeneration of the optic nerve in adult zebrafish. Glia 60:253-270.
Münzel EJ, Becker CG, Becker T, Williams A (2014) Zebrafish regenerate full thickness optic nerve myelin after demyelination, but this fails with increasing age. Acta Neuropathol Commun 2:1-14.
Nawaz S, Schweitzer J, Jahn O, Werner HB (2013) Molecular evolution of myelin basic protein, an abundant structural myelin component. Glia 61:1364-1377.
Neely SA, Williamson JM, Klingseisen A, Zoupi L, Early JJ, Williams A, Lyons DA (2022) New oligodendrocytes exhibit more abundant and accurate myelin regeneration than those that survive demyelination. Nat Neurosci 25:415-420.
Negintaji K, Ghanbari A, frozanfar M, Jafarinia M, Zibara K (2023) Pregnenolone enhances the proliferation of mouse neural stem cells and promotes oligodendrogenesis, together with Sox10, and neurogenesis, along with Notch1 and Pax6. Neurochem Int 163:105489.
Ohtomo R, Iwata A, Arai K (2018) Molecular mechanisms of oligodendrocyte regeneration in white matter-related diseases. Int J Mol Sci 19:1743.
Ohtomo R, Arai K (2020) Recent updates on mechanisms of cell-cell interaction in oligodendrocyte regeneration after white matter injury. Neurosci Lett 715:134650.
Park HC, Mehta A, Richardson JS, Appel B (2002) olig2 is required for zebrafish primary motor neuron and oligodendrocyte development. Dev Biol 248:356-368.
Parrilla M, Lillo C, Herrero-Turrion MJ, Arévalo R, Lara JM, Aijón J, Velasco A (2009) Pax2 in the optic nerve of the goldfish, a model of continuous growth. Brain Res 1255:75-88.
Parrilla M, León-Lobera F, Lillo C, Arévalo R, Aijón J, Lara JM, Velasco A (2016) Sox10 expression in goldfish retina and optic nerve head in controls and after the application of two different lesion paradigms. PLoS One 11:e0154703.
Perdikaris P, Prouska P, Dermon CR (2023) Social withdrawal and anxiety-like behavior have an impact on zebrafish adult neurogenesis. Front Behav Neurosci 17:1244075.
Pérez-Montes C, Jiménez-Cubides JP, Velasco A, Arévalo R, Santos-Ledo A, García-Macia M (2023) REDOX balance in oligodendrocytes is important for zebrafish visual system regeneration. Antioxidants (Basel) 12:2026.
Pingault V, Zerad L, Bertani-Torres W, Bondurand N (2022) SOX10: 20 years of phenotypic plurality and current understanding of its developmental function. J Med Genet 59:105-114.
Rupprecht J, Reiprich S, Baroti T, Christoph C, Sock E, Fröb F, Wegner M (2024) Transcription factors Sox2 and Sox3 directly regulate the expression of genes involved in the onset of oligodendrocyte differentiation. Cells 13:935.
Santos E, Yanes CM, Monzón-Mayor M, del Mar Romero-Alemán M (2006) Peculiar and typical oligodendrocytes are involved in an uneven myelination pattern during the ontogeny of the lizard visual pathway. J Neurobiol 66:1115-1124.
Santos-Ledo A, Pérez-Montes C, DeOliveira-Mello L, Arévalo R, Velasco A (2023) Oligodendrocyte origin and development in the zebrafish visual system. J Comp Neurol 531:515-527.
Shinozaki Y, Namekata K, Guo X, Harada T (2024) Glial cells as a promising therapeutic target of glaucoma: beyond the IOP. Front Ophthalmol (Lausanne) 3:1310226.
Sock E, Wegner M (2021) Using the lineage determinants Olig2 and Sox10 to explore transcriptional regulation of oligodendrocyte development. Dev Neurobiol 81:892-901.
Song H, Wang D, De Jesus Perez F, Xie R, Liu Z, Chen CC, Yu M, Yuan L, Fernald RD, Zhao S (2017) Rhythmic expressed clock regulates the transcription of proliferating cellular nuclear antigen in teleost retina. Exp Eye Res 160:21-30.
Stella SL, Geathers JS, Weber SR, Grillo MA, Barber AJ, Sundstrom JM, Grillo SL (2021) Neurodegeneration, neuroprotection and regeneration in the zebrafish retina. Cells 10:633.
Takada N, Appel B (2010) Identification of genes expressed by zebrafish oligodendrocytes using a differential microarray screen. Dev Dyn 239:2041-2047.
Thorburne SK, Juurlink BH (1996) Low glutathione and high iron govern the susceptibility of oligodendroglial precursors to oxidative stress. J Neurochem 67:1014-1022.
Ulloa-Navas MJ, Pérez-Borredá P, Morales-Gallel R, Saurí-Tamarit A, García-Tárraga P, Gutiérrez-Martín AJ, Herranz-Pérez V, García-Verdugo JM (2021) Ultrastructural characterization of human oligodendrocytes and their progenitor cells by pre-embedding immunogold. Front Neuroanat 15:696376.
Van houcke J, Bollaerts I, Geeraerts E, Davis B, Beckers A, Van Hove I, Lemmens K, De Groef L, Moons L (2017) Successful optic nerve regeneration in the senescent zebrafish despite age-related decline of cell intrinsic and extrinsic response processes. Neurobiol Aging 60:1-10.
Wegner M, Stolt CC (2005) From stem cells to neurons and glia: A Soxist's view of neural development. Trends Neurosci 28:583-588.
Wegner M (2008) A matter of identity: Transcriptional control in oligodendrocytes. J Mol Neurosci 35:3-12.
Won MH, Kang TC, Cho SS (2000) Glial cells in the bird retina: Immunochemical detection. Microsc Res Tech 50:151-160.
Xiao Y, Petrucco L, Hoodless LJ, Portugues R, Czopka T (2022) Oligodendrocyte precursor cells sculpt the visual system by regulating axonal remodeling. Nat Neurosci 25:280-284.
Zhang T, Bhambri A, Zhang Y, Barbosa D, Bae HG, Xue J, Wazir S, Mulinyawe SB, Kim JH, Sun LO (2023a) Autophagy collaborates with apoptosis pathways to control oligodendrocyte number. Cell Rep 42:112943.
Zhang Y, Zhao Q, Chen Q, Xu L, Yi S (2023b) Transcriptional control of peripheral nerve regeneration. Mol Neurobiol 60:329-341.
Zhou L, McAdow AR, Yamada H, Burris B, Shaw DK, Oonk K, Poss KD, Mokalled MH (2023) Progenitor-derived glia are required for spinal cord regeneration in zebrafish. Development 150:dev201162.

C-Editor: Zhao M; S-Editor: Li CH; L-Editors: Li CH, Song LP; T-Editor: Jia Y

斑马鱼视神经再生涉及定居性和视网膜来源的少突胶质细胞
文章特色分析

一、文章重要性

1. 揭示斑马鱼视神经再生的细胞机制

斑马鱼作为中枢神经系统再生的经典模型，其视神经在损伤后能完全再生。本研究明确了少突胶质细胞在这一过程中的关键作用，填补了关于其来源、命运转变与功能调控的认知空白。

2. 为哺乳动物神经再生研究提供借鉴

与哺乳动物不同，斑马鱼在损伤后能有效清除受损少突胶质细胞并再生新的髓鞘形成细胞。这一机制的理解，有助于揭示为何哺乳动物中枢神经系统再生能力有限，并为促进其再生提供潜在靶点。

3. 强调胶质细胞在再生中的主动角色

研究突破了传统上认为胶质细胞仅是“支持细胞”的观念，展示了少突胶质细胞在轴突导向、营养支持与髓鞘再生中的主动调控作用。

二、创新性特色

1. 首次系统追踪少突胶质细胞在视神经再生中的时空动态

- 使用 sox10:tagRFP 转基因斑马鱼 结合 Sox2 免疫组化，清晰区分成熟少突胶质细胞与干细胞/前体细胞。

- 时间点覆盖从损伤后 6 小时至 14 天，完整捕捉了从退化到再生的全过程。

2. 提出“两波少突胶质细胞分化”模型

- 第一波（早期）：来自视神经内定居的 Sox2+ OPCs，在 24–72 hpl 开始分化为 sox10+ 少突胶质细胞。

- 第二波（晚期）：来自视网膜内（如 ONFL、INL）的 Sox2+ 干细胞，在 7–14 dpl 参与再生。

3. 揭示少突胶质细胞的非典型死亡机制

- 发现损伤后 sox10+ 细胞虽消失，但不通过典型凋亡途径（TUNEL 阴性），提示可能存在自噬或其他非经典死亡方式。

4. 明确视网膜来源的少突胶质细胞参与再生

- 发现视网膜内（尤其是 ONFL）的 Sox2+ 细胞也能分化为少突胶质细胞，并迁移至损伤部位，支持轴突再生与髓鞘形成。

三、对学科的启示

1. 推动“胶质细胞可塑性”研究

本研究显示，少突胶质细胞在损伤后表现出显著的形态与功能可塑性，这为理解胶质细胞在神经系统修复中的多重角色提供了新视角。

2. 为治疗哺乳动物中枢神经损伤提供新思路

斑马鱼能够有效清除损伤少突胶质细胞并再生新的细胞，而哺乳动物则形成胶质瘢痕阻碍再生。研究提示：促进损伤少突胶质细胞的清除与新细胞的生成，可能是促进哺乳动物中枢神经再生的关键策略。

3. 强调干细胞/前体细胞在再生中的时空特异性

不同来源（视神经内 vs 视网膜内）的 Sox2+ 细胞在不同时间点参与再生，提示再生治疗需考虑细胞来源与时机。

4. 推动非凋亡性细胞死亡机制研究

研究提出少突胶质细胞可能通过自噬等方式死亡，这为神经退行性疾病与损伤修复中的细胞死亡机制研究开辟了新方向。

总结

该研究通过高分辨率时空追踪与多标记分析，系统揭示了斑马鱼视神经再生中少突胶质细胞的动态变化、来源及其功能转变，提出了“两波再生”模型，并揭示了其非典型死亡机制。这些发现不仅深化了对中枢神经系统再生机制的理解，也为哺乳动物神经再生策略的开发提供了重要的理论依据与实验基础。